

MHD models of Pulsar Wind Nebulae

Niccolò Bucciantini

Abstract Pulsar Wind Nebulae (PWNe) are bubbles or relativistic plasma that form when the pulsar wind is confined by the SNR or the ISM. Recent observations have shown a richness of emission features that has driven a renewed interest in the theoretical modeling of these objects. In recent years a MHD paradigm has been developed, capable of reproducing almost all of the observed properties of PWNe, shedding new light on many old issues. Given that PWNe are perhaps the nearest systems where processes related to relativistic dynamics can be investigated with high accuracy, a reliable model of their behavior is paramount for a correct understanding of high energy astrophysics in general. I will review the present status of MHD models: what are the key ingredients, their successes, and open questions that still need further investigation.

1 Introduction

When the ultra-relativistic wind from a pulsar interacts with the ambient medium, either the SNR or the ISM, a bubble of non-thermal relativistic particles and magnetic field, known as Pulsar Wind Nebula or “Plerion” (PWN), is formed. The Crab Nebula is undoubtedly the best example of a PWN, and it is often considered the prototype of this entire class of objects, to the point that models of PWNe are, to a large extent, based on what is known in this single case. The first theoretical model of the structure and the dynamical properties of PWNe was presented by Rees & Gun [88], further developed in more details by Kennel & Coroniti [64, 65] (KC84 hereafter), and is based on a relativistic MHD description.

The MHD paradigm is based on three key assumptions:

N. Bucciantini
NORDITA, Roslagstullsbacken 23, 106 91 Stockholm, Sweden, e-mail:
niccolo@nordita.org

- that the larmor radii of the particles is much smaller than the typical size of the nebula, and particles are simply advected with the magnetic field. This is true up to energies of order of the pulsar's voltage, where the larmor radius becomes comparable with the typical size of the system.
- That radiative losses are negligible, or at least that they can be accounted for by renormalizing the pulsar spin-down luminosity. This again can be proved to be true in the case of Crab Nebula (and to some extent also in other systems with good spectral coverage), where the synchrotron spectrum shows that the particles carrying the bulk of the energy have a typical lifetime for synchrotron cooling longer than the age of the nebula.
- That we are dealing with almost pure pair plasma, and dispersive or hybrid effects (separation of scales) due to the presence of heavier ions are absent. While there is no direct evidence for the absence of ions, standard pulsar wind theory, and the success of the MHD model of PWNe suggest that, from a purely dynamical point of view, there is no need for this extra component.

In its simplest form [88] the MHD model of PWNe can be summarized as follows (see Fig. 3): the ultra-relativistic pulsar wind is confined inside the slowly expanding SNR, and slowed down to non-relativistic speeds in a strong termination shock (TS). At the shock the plasma is heated, the toroidal magnetic field of the wind is compressed, and particles are accelerated to high energies. These high energy particles and magnetic field produce a post-shock flow which expands at a non-relativistic speed toward the edge of the nebula.

Despite its simplicity the MHD model can explain many of the observed properties of PWNe, and until now no observation has been presented that could rule it out. The presence of an under-luminous region, centered on the location of the pulsar, is interpreted as due to the ultra-relativistic unshocked wind. Polarization measures [112, 106, 93, 57, 82, 42, 70, 53] show that emission is highly polarized and the nebular magnetic field is mostly toroidal, as one would expect from the compression of the pulsar wind, and it is consistent with the inferred symmetry axis of the system. The pressure anisotropy associated to the compressed nebular toroidal magnetic field [11, 101], explains the elongated axisymmetric shape of many PWNe (*i.e.* Crab Nebula, 3C58). The MHD flow from the TS to the edge of the nebula also leads to the prediction that PWNe should appear bigger at smaller frequencies: high energy X-rays emitting particles are present only in the vicinity of the TS, having a shorter lifetime for synchrotron losses, compared to Radio particles which fill the entire volume, having negligible losses on the age of the nebula. This increase in size at smaller frequencies is observed in the Crab Nebula [105, 14, 7].

However one must bear in mind that not all properties of PWNe can be explained within the MHD framework, which, ultimately, only provides a description of the flow dynamics. For example, the acceleration of particles at the TS that accounts for the continuous, non-thermal, very broad-band spectrum, extending from Radio to X-rays [105, 8, 110, 111, 83], is usually assumed as given. The MHD model provides no hint to the reason why the injection spectrum looks like a broken power law, with no sign of a Maxwellian component at lower energies. Moreover the MHD description might prove faulty if applied to particles responsible for the emission in

the 10-100 MeV band, whose larmor radii are comparable to the size of the TS, and can lead to wrong conclusion on their expected behavior.

The MHD model of PWNe has been used, by comparing observations with the predictions of numerical simulations, to constrain some of the properties of the pulsar wind, at least at the distance of the TS. While it is not possible to derive the Lorentz factor of the wind, or its multiplicity, it is possible to constrain the ratio between Poynting flux and kinetic energy, the latitudinal dependence of the energy flux, and the presence of a dissipated equatorial current sheet. This shows that nebular properties can be used to derive informations on the conditions of the pulsar wind at large distances.

2 Jet-Torus structure and Inner flow properties

Let start our discussion from young objects. The Crab Nebula, 3C58, MSH 15-52, G21.5 all belongs to this group. Younger objects are the most well studied and perhaps the ones for which the MHD models have provided the greatest insight. These systems are characterized by a simple interaction with the confining SNR, they are bright, we have broad band data, and the pulsar proper motion can be neglected. Older systems are often subject to a much more complex interaction with the SNR, they are affected by the pulsar proper motion, and usually lack the deep observational coverage of the younger counterparts. For this reasons, models of old objects have also progressed far less than for young ones, and the agreement with observations is mostly qualitative. We will leave a description of MHD models of the evolution of PWNe to Sec. 3.

The KC84 model has been for a long time the reference for the understanding of young PWNe, with only minor theoretical developments. Things have changed recently thanks to high resolution optical and X-rays images from HST, CHANDRA and XMM-Newton, that have have shown that the properties of the emission at high energy cannot be explained within a simplified one dimensional model. This refers not just to the geometrical features that are observed, but in practice to all aspect of X-ray emission.

These new data show that the inner region of young PWNe is characterized by a complex axisymmetric structure, generally referred as *jet-torus structure* (Fig. 2). First observed in Crab [54, 110], it has subsequently been detected in many other PWNe [50, 44, 52, 87, 45, 74, 91, 95, 35, 92], to the point that the common consensus is that, with deep enough observations, it should always be detected. This structure is characterized by an emission torus, in what is thought to be the equatorial plane of the pulsar rotation, and, possibly, a series of multiple arcs or rings, together with a central knot, almost coincident with the pulsar position, and one or two opposite jets along the polar axis, which seem to originate close to the pulsar itself. Even if the existence of a main torus could be qualitatively explain as a consequence of a higher equatorial energy injection [20] it is not possible to reproduce quantitatively the observed luminosity. Shibata et al. [94] were the first to point that,

the difference in brightness between the front and back sides of the torus in Crab Nebula, requires a post-shock flow velocity $\sim 0.4 - 0.5c$, much higher than what expected for subsonic expanding flows. The same conclusion applies to all the other systems where a torus is observed. The existence of an inner ring, detached from the torus, and of the knot which seemed to be located inside the wind region, are incompatible with the assumption of a smooth flow from the TS. From a theoretical point of view however, the most interesting feature is the jet [78], because theoretical [12, 13] and numerical [34, 19, 51, 68, 30] studies of relativistic winds from pulsars have shown no presence of collimated energetic outflow. To this, one must add other observed properties, like the X-rays photon index maps of Crab Nebula, Vela and Kes 75 [83, 61, 85], which hardens moving from the inner ring toward the main torus, while steepening due to synchrotron losses is expected, and the relatively large size of the X-ray nebula in Crab compared to the radio [4]. The fact that the symmetry axis of the jet-torus corresponds to the major axis of the nebula, leads immediately to the conclusion that the toroidal magnetic field is paramount in shaping the inner flow.

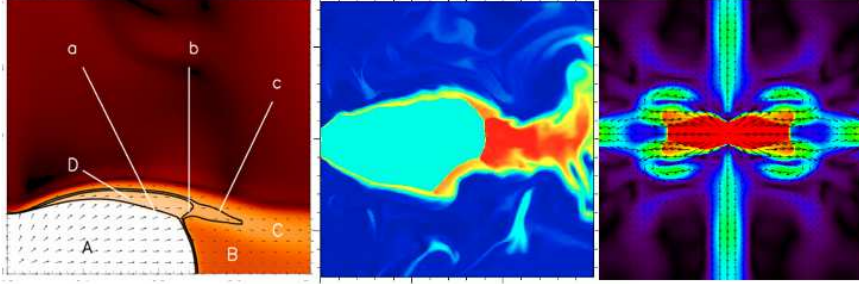


Fig. 1 From left to right: structure of the post shock flow in PWNe [40], the funneling of the wind (A) into an equatorial flow (B/C) is clearly evident. Same structure showing the complex flow dynamics that develops downstream of the shock and the corrugation of the shock surface which manifests itself as time variability at high energy [33]. Numerical result of the internal dynamics in the body of the PWN [40] where the flow is diverted back toward the axis by the magnetic hoop stresses, and is collimated into a jet.

The keys in understanding the jet-torus structure are the magnetization and energy distribution in the pulsar wind. It has been known for a long time [81], and has been recently confirmed with numerical simulations [19, 68, 30], that far from the Light Cylinder a higher equatorial energy flux is expected. It is this particular latitudinal distribution of the pulsar spin-down luminosity which naturally produces an oblate TS with a cusp in the polar region [20, 21], giving rise to a complex post-shock dynamics. The obliquity of the TS at higher latitudes, forces the flow in the nebula toward the equator with speeds $\sim 0.3 - 0.5c$. Hoop-stresses are more efficient in the mildly relativistic flow, and the collimation of a jet occur in the post shock region [75, 63]. The evident complexity of this scenario makes clear that the only possible way to proceed require the use of efficient and robust numerical schemes

for relativistic MHD [67, 39, 48]. Thanks to numerical simulations this qualitative picture has been developed into a quantitative model which has been successfully validated against observations.

The starting point of the MHD model is the structure of the force-free pulsar wind: the energy flux in the wind has a strong latitudinal dependence of the form $L(\theta) = L_o(1 + \alpha \sin(\theta))$, where α is a measure of the pole-equator anisotropy, while the magnetic field in the wind $B(\theta) \propto \sin(\theta)$. Various numerical simulations of the interaction of such wind with the SNR ejecta have been presented [69, 40, 22, 41, 109, 33]: the result of the anisotropic energy distribution in the wind is that almost all of the downstream plasma is deflected toward the equatorial plane, and flow channels with velocity $\sim 0.5c$ can form, the value expected in order to justify the luminosity distribution in the torus of the Crab Nebula [94]. Shear and instabilities tend to destroy this collimated equatorial flow before it reaches the edge of the nebula, however a bulk equatorial motion survives to distances corresponding to the location of the torus. It is this flow inside the nebula, with speed in excess of $c/3$ that advect freshly injected particles to larger distances, giving rise to a more extended X-ray nebula, that the simple 1D model would predict[4]. The post shock flow is independent on the specific values of Lorentz factor or density distribution, but it is only determined by the pulsar spin-down energy distribution, and the nebular dynamics cannot be used to constrain the value of the wind Lorentz factor or the multiplicity in the wind.

As the flow expands away from the TS, toward the edge of the nebula, the magnetization increases, until equipartition is reached. Due to the magnetic field distribution in the wind, equipartition is first reached close to the equator than at higher latitudes. The magnetic pressure prevents further compression beyond equipartition, hoop stresses in the mildly relativistic postshock flow become efficient, and the flow is diverted back toward the axis. This is the process that causes the formation of a collimated jet along the axis itself. The wind magnetization regulates the formation and properties of the jet: for low values $\sigma < 0.001$, equipartition is not reached inside the nebula, and no jet is formed. At higher magnetizations equipartition is reached in the close vicinity of the TS, and most of the plasma ends in a jet. The plasma speed in the jet is $\sim 0.7c$, in agreement with observation of the jet in Crab Nebula and MSH 15-52 [110, 56, 72, 38], for magnetization values $\sigma \sim 0.1$. Associated with this collimated back-flow there is a global circulation inside the nebula, with typical speeds $\sim 0.1c$ that might lead to mixing with cold ions [80].

Numerical models offer the possibility to investigate different distributions of magnetic field in the wind. In particular, for oblique rotators, while the energy distribution in the wind is identical to the aligned case [18, 96], the magnetic field is supposed to give rise to a striped equatorial region, with alternating polarities. If this striped wind region is dissipated, and this can happen either in the wind [79, 66] or at the termination shock itself [76, 77], then a low magnetization equatorial flow is expected, which adds complexity to the flow structure inside the nebula. One of the main success of the MHD model is that emission maps based on the results of numerical simulations give different observational signatures if an unmagnetized equatorial sector, corresponding to the striped wind region, is present or not: a large

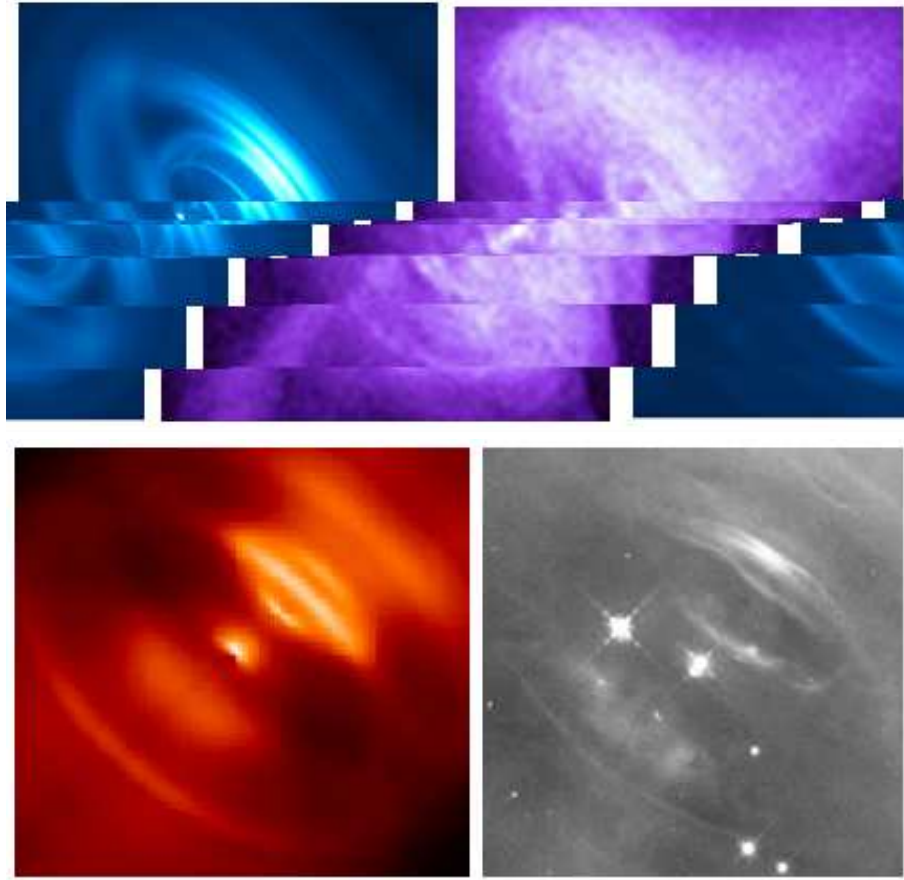


Fig. 2 Upper panel: left - simulated X-rays synchrotron map based on numerical MHD simulations of the flow [33]; right - CHANDRA image of the central region of Crab Nebula. The two images have similar scaling. Lower panel: left - simulated optical synchrotron map based on numerical MHD simulations of the flow (different from the above one); right - HST image of the wisp region in Crab Nebula [56]. Note the agreement between the observed features and the results of MHD models.

striped region is needed to explain the observed inner-ring outer-torus structure of many PWNe, while models without it lead to single ring nebulae.

When comparing observations with emission maps based on the fluid structure derived from relativistic MHD simulations we clearly see that, within the MHD regime, it is possible to recover almost all of the observed features, with correct size and luminosity. However, until now, little work has been devoted to investigate if it is possible to discriminate among various particle injection mechanisms. Work has mostly focused on X-ray, and a uniform injection in the form of a single power-law distribution has been assumed [41, 109, 69, 33]. Moreover one should be aware

that even today, with better computational facilities, it is not possible to conduct an exhaustive sampling of the entire parameter space characterizing the interaction of PWNe with SNRs. Works has mostly focused on reproducing Crab Nebula, where many parameters are constrained by a rich set of observations.

In Fig. 2, CHANDRA and HST images of the Crab Nebula are compared to maps based on a simulations with striped wind in X-rays and optical. The knot and the inner ring are both present, and they are due to the high velocity flow in the immediate post shock region, at intermediate latitudes. The main torus is visible at larger distances, as well as features like the *anvil* which corresponds to the backward side of the nebula. X-ray maps of the spectral index based on simulations also agree with the main observed properties of the Crab Nebula [83] and with recent results about Vela [61] and Kes 75 [85]: in particular the spectrum appears to flatten moving away from the pulsar toward the main torus, without the need to assume any re-acceleration. All this rich emission pattern is ultimately related to Doppler boosting effects: at high speed, the emission is enhanced (rings) and the spectrum is harder. There are still problems to recover the correct luminosity/spectrum in the jet. This might be indicative of some form of dissipation and re-energization along the axis; possibly associated with local instabilities in the toroidal magnetic field [9] which present axisymmetric simulations cannot address, but for which there are many observational evidences [87, 84, 72, 38].

Preliminary results [33] show that, to realistically reproduce the X-ray emission from Crab Nebula, $\sigma \simeq 0.1$ is required (about two orders of magnitude higher than the 1D estimate by KC84) in conjunction with a large ($\sim 45^\circ$) striped zone.

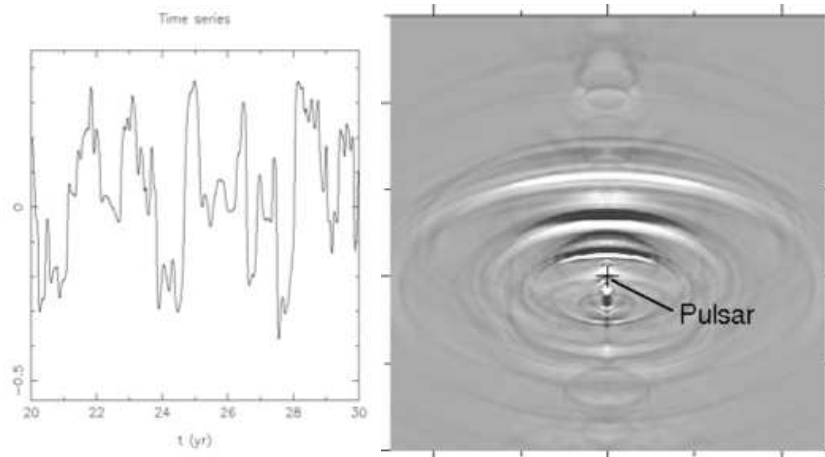


Fig. 3 Variability in the wisps region in MHD [33]. Left figure: variability at a selected point on axis, note the typical 2-years long cycle and also the shorter timescale variations. Right figure: variability of the nebula obtained by subtracting two images at 2-year distance. The outgoing wave pattern is easily seen. Compare with optical images from [56].

Perhaps the most promising clues to investigate the flow dynamics inside PWNe in the future might come from polarization, and possibly X-ray polarization: while emission maps mostly trace the flow velocity inside the nebula, they have little sensitivity to the presence of a small scale disordered component of the magnetic field. There are several indications from optical polarimetry in the Crab Nebula [53], as well as indication from recent MHD simulations [33, 109], suggesting that turbulence might be present, in the body of the nebula, leading to a partial randomization of the field. The effect of the flow velocity on the polarization angle has been discussed by [29] and [41], and the results generally agree with available optical polarization measured in Crab [112, 106, 93, 57, 53].

2.1 Time variability

It is known that, close to the supposed location of the termination shock, PWNe show a short time variability mainly detected in optical and X-ray bands. This however does not affect the global properties of the main observed features belonging to the jet-torus structure (i.e. the inner ring, torus and jet) which appear to be quite persistent on long time-scales. Variability of the wisps in the Crab Nebula has been known for a long time [56, 15]. Recent observations have shown that the jet in Vela appears to be strongly variable [86, 87], together with the main rings [61]. Variability is also observed in the jet of Crab [84, 72], and has recently been detected in MSH 15-52 [38].

In the strongly toroidal field of these nebulae, the jet variability, which usually has a time-scale of years, is likely due to kink or sausage mode, or even to fire-hose instability [100]. On the other hand the wisps show variability on shorter time-scales of months: the variability takes the form of an outgoing wave pattern, with a possible year-long duty cycle.

For a long time the only model capable of reproducing the observed variability was the one proposed by Spitkovsky & Arons [97], based on the assumption that ions are present in the wind. The idea of ions was also supported by kinetic simulations of acceleration in a strong shock [3]. The presence of particles with Larmor radii, of order of the size of termination shock, introduces kinetic effects related to the separation of scales, leading to compression of electrons. The model however requires a large fraction of pulsar spin-down energy in the ion component, which contrasts the basic idea of leptonic dominated systems, and in general is not supported by spectral models of PWNe.

The most recent achievement of the MHD nebular models has been the ability to reproduce the observed variability [33, 31, 10, 109]. It is the fundamental multidimensional nature of the problem that allows for variability of the flow pattern. It was already noted in early simulations [22] that the synchrotron emissivity inside the nebula varies. There were also evidences [69] suggesting that the nebular flow might have a feedback action on the TS, causing it to change shape, and thus inducing a change in the appearance of the wisps.

This picture has been confirmed recently [33, 109]: within the MHD regime it is possible to recover the variability, the outgoing wave pattern, its typical speed, and luminosity variations. It is found indeed that a SASI like instability is present. Waves injected at the termination shock can propagate toward the axis, feeding back on the termination shock and triggering the injection of new waves. Simulations show that there is a typical duty-cycle of about 1-2 year; more generally the duty-cycle will be of the order of the radius of the termination shock divided by the typical propagation speed $\sim 0.5c$.

2.2 *Gamma rays*

At the moment the most promising observational avenue in PWNe research is the study of gamma-ray emission. HESS has shown that many extended gamma-ray sources are associated with PWNe both young ones in the free expansion phase and older ones undergoing reverberation [36, 47]. New results from the FERMI satellite are just arriving [1, 2], with data extending from the high energy MeV synchrotron part of the spectrum, to the 100 GeV IC part.

The emission at MeV energy observed from young object should enable us to put constraints on the acceleration mechanism. It seems that an exponential cutoff in energy can explain the observed data. The more interesting question regard how the observed variability of the wisps manifest itself at higher energies. Naively one might expect that the emission at high energies should show similar variability, on comparable time-scales, but with amplitudes of order unity. On the other hand preliminary results [73] suggest that in the 100MeV range no variability is detected. This has important implications in term of acceleration: particles responsible for the 100MeV emission have typical larmor radii of order of the size of the TS. Coincidentally this is also the coherent length of the turbulence that is at the base of the MHD variability [33]. In this sense high energy particles, are decoupled from the MHD flow, and their response to the MHD turbulence is incoherent. This of course deserves further investigation. In particular one would like to know at what energy variability reaches a maximum, where the particles start to decouple from the MHD flow, and to what degree this incoherent interaction with turbulence can induce variability.

The emission at GeV energies is assumed to be from Inverse Compton scattering on background radiation, and in the case of Crab the self synchrotron. Interestingly the spectral properties of the comptonized radiation can be used to derive information about particles which are supposed to emit synchrotron in the UV, and are usually not directly accessible given the high UV absorption in the ISM. In the case of MSH 15-52 [2] Fermi results, have ruled out previous EGRET measures, and shown that the undetected high energy part of the particle distribution function must be harder than previously assumed. Similar results could be expected for Kes 75. GeV emission could in principle help provide an independent constraint on the magnetization in the nebula.

An alternative contribution to the gamma ray emission, if protons are present in the pulsar wind, is the p-p scattering and related pion decay [5, 59]. However uncertainties on the target number density and the spin-down energy in protons, make this channel hard to constrain. At present IC scattering can fit most of the objects, if one allows for fluctuations of the local background of order unity with respect to the galactic average.

Recently a series of simplified evolutionary models for the high energy emission from PWNe have been developed extending beyond the free expansion [37, 49, 32]. This is quite important given that the majority of the gamma-ray PWNe are supposed to be post-reverberation objects, where the interaction with the SNR shell can play a major role

For example in many of these objects the bulk of the gamma emission is not centered on the pulsar, and the displacement is too large to be explained in term of a moving pulsar leaving behind a relic PWN. Two possible explanations have been invoked: an off-center compression by the reverse shock [16]; or the formation of a bow-shock tail [28, 62], where particle responsible for the inverse Compton emission in the gamma-ray band can be advected to large distances from the pulsar.

3 Evolution of PWNe

In the previous section we have devoted our attention to the successes of the fluid/MHD model regarding the emission properties observed in young system. Numerical simulations offer also a way to follow the evolution of a PWN and its interaction with the SNR at later ages.

At the moment, however, the study of old object has been limited to a qualitative analysis of the interaction in an attempt to recover the main phases of the evolution and understand how the observed multi-wavelength morphology depends on the interaction itself.

In the analytic model developed by KC84 the SNR has only a passive role, providing the confinement of the PWN. Given the complexity of the PWN-SNR interaction, a detailed study of the evolution of the system, has been possible only recently, thanks to the improvement in computational resources [102, 16, 25, 104, 43].

By comparing the energy in the SNR ($\sim 10^{51}$ ergs) to the total energy injected by the pulsar during its lifetime ($\sim 10^{49}$ ergs) it is easy to realize that a PWN cannot significantly affect the SNR, while the evolution of the SNR can have important consequences for the PWN.

There are three main phases (for a more complete discussion of PWN-SNR evolution see [89] and [46]), in the PWN-SNR evolution. At the beginning the PWN expands inside the cold SN ejecta. The SN ejecta are in free expansion, so this phase is generally called *free expansion phase*. This phase lasts for about 1000-3000 yr, and during this period the pulsar luminosity is high and almost constant. This is the present phase of the Crab Nebula, 3C58, MSH 15-52, G21.5, and PWNe in this phase are expected to shine in high energy X-rays emission. The expansion velocity

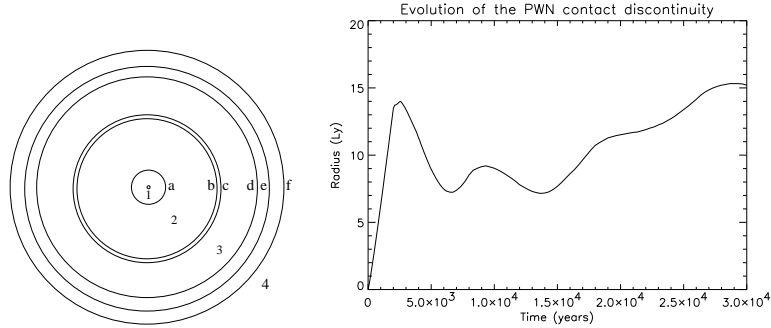


Fig. 4 Left picture: schematic representation of the global structure of the PWN in the first phase of its evolution inside a SNR. From the center the various regions are: 1- the relativistic pulsar wind, 2- the hot magnetized bubble responsible for the non thermal emission, 3- the free expanding ejecta of the SNR, 4- the ISM. These regions are separated by discontinuities: a- the wind termination shock, b- the contact discontinuity between the hot shocked pulsar material and the swept-up SNR ejecta, c- the front shock of the thin shell expanding into the ejecta, d- the reverse shock of the SNR, e- the contact discontinuity separating the ejecta material from the compressed ISM, f- the forward SNR shock. Right picture: evolution of the PWN size, from free-expansion to sedov phase (from [25]).

of PWNe in this early stage is typically few thousands kilometer per second. For this reason one can neglect the pulsar kick (velocities in the range 50-300 km/s) in modeling young objects, and assume the pulsar to be centrally located. As the system expands inside the high density, cold, supersonic ejecta of the SNR, a thin shell of swept-up material is formed. Given that the density of the shell is much higher than the enthalpy of the relativistic plasma, the shell is subject to Rayleigh-Taylor instability. This is supposed to be at the origin of the filamentary network of the Crab Nebula [55, 60, 27], and 3C58 [17]. In the thin-shell approximation, it has been shown that it is possible to derive an analytic self-similar solution [27], describing the expansion of the nebula in this phase.

The PWN will expand until eventually it will come into contact with the reverse shock in the SNR shell. In the absence of a central source of energy, like a pulsar, the reverse shock is supposed to recede to the center of the SNR in a time of order of 5000-10000 yr [99]. From this moment on the evolution of the PWN is modified by the more massive and energetic SNR shell: the PWN undergoes a compression phase generally referred as *reverberation phase*, that can last 5000-10000 yr. In the simple 1D scenario the pressure in the compressed PWN will rise to balance the compression and to push back the ejecta, and the nebula might undergo several compression and rarefaction cycles. This is however an artifact of the 1D geometry, and conclusion based on the existence of these oscillations are not reliable. More appropriate multidimensional studies have shown that the SNR-PWN interface is highly Rayleigh-Taylor unstable during compression [16], which can cause efficient mixing of the pulsar wind material with the SNR. This mixing will most likely prevent any oscillation and the system might rapidly relax to pressure equilibrium. This reverberation phase is supposed to last about 10^4 years. Even if

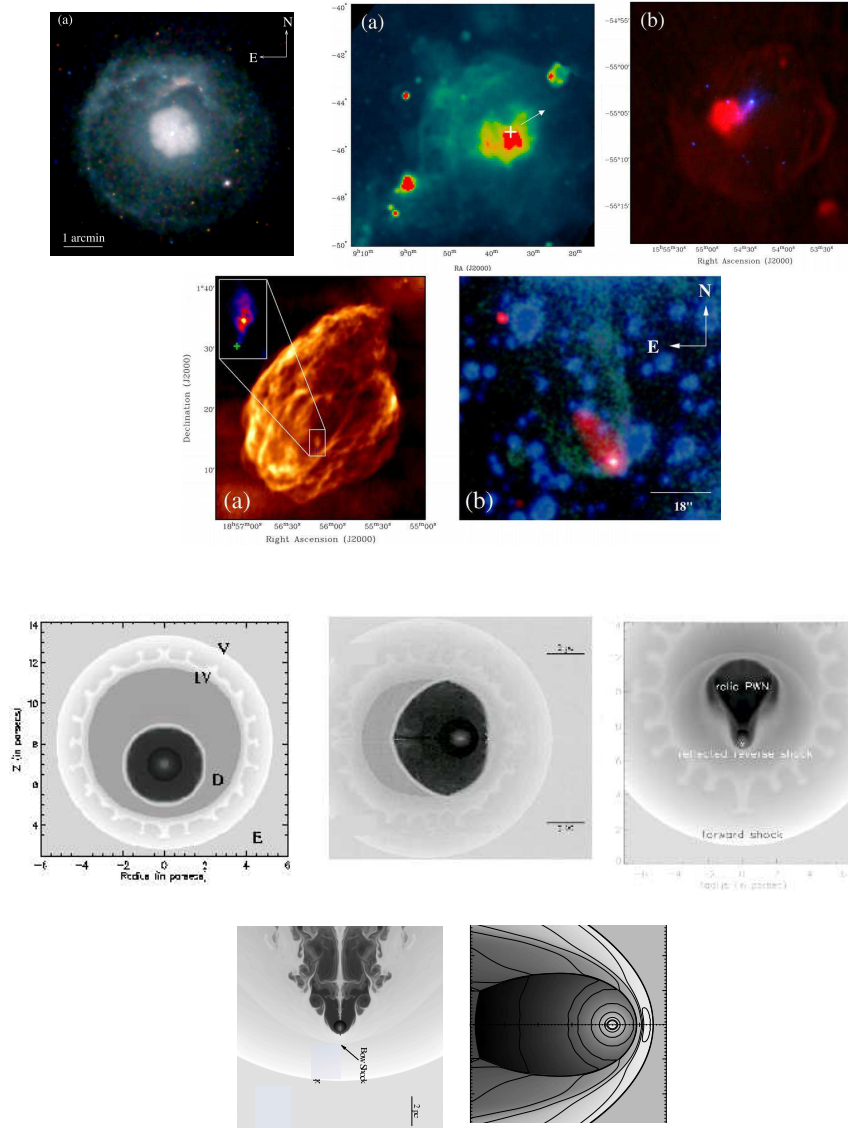


Fig. 5 Upper part: images of various evolutionary phases of PWNe (from Gaensler & Slane [46]). From Left to right, up to down: X-ray image of the composite remnant G21.5-0.9, free expansion phase; radio image of Vela SNR, displacement of the nebula due to the compression of the reverse shock during reverberation; SNR G 327.1-1.1 in radio (red) and X-rays (blue), relic PWN phase; W44 in radio, transition to the internal bow-shock phase; PSR B1957+20 in $H\alpha$ (green) an X-rays (red), ISM bow-shock nebula. Lower part: numerical hydrodynamical simulations of the various phases of the PWN-SNR evolution (from [104, 23]). Each figure of the lower part corresponds to systems shown in the upper one.

energy injection from the pulsar at these later times is negligible, PWNe can still be observed, due to the re-energization during compression. The interaction with the reverse shock can lead to a variety of different morphological structures if one consider also the pulsar proper motion [103, 104, 28, 43]. The most likely outcome of the interaction is that the nebula can be displaced with respect to the location of the pulsar. At the beginning this might result into a system where the pulsar is not located at the center of the radio non thermal emission, analogous to what is observed in Vela. As the system evolves the reverse shock will completely displace the body of the PWN, creating a relic nebula. The relic PWN will mostly contain low energy particles, and will be visible in radio, while high energy particles, observable in X-rays will be seen only close to the pulsar. G327.1 shows indeed this kind of morphology [46]. Depending on projection effects one might also end up with very small X-ray nebulae centered on vast and large radio nebulae. In this regard polarization might prove essential to disentangle the structure. In particular, if the Rayleigh-Taylor instability is efficient and the radio nebula is disrupted and mixed with the ejecta, one expects to find a low level of polarization and no evidence for a global toroidal field. To this one must add the possibility that the ISM magnetic field might be dragged inside the PWN, or the nebular field inside the SNR shell. Given the importance of magnetic configurations for particle (cosmic ray) diffusion, one understands how important a proper model of older objects is.

At later time the SNR ejecta starts cooling and the pulsar will eventually become supersonic. Once this happen the pulsar will form around itself a bow-shock PWN, and one expects an emission tail to form connecting the pulsar to the relic PWN. This model apply to the morphology and structure of W44 [46], or possible IC443. Interestingly, the location with respect to the SNR where this happens does not depend on the pulsar proper motion, and turns out to be $\sim 70\%$ of the radius of the forward shock. An obvious question is if the jet-torus structure, that is observed in young and relatively undisturbed systems, can survive the later interaction with the SNR shell and the reverse shock. We know that in Vela the jet-torus is visible and does not appear to be distorted, this suggest that, as long as the evolution is subsonic, in the pulsar vicinity the dynamic of the nebula flow will still be regulated by the pulsar wind. On the other hand bow-shock simulations have shown that the typical size of the nebula in the head of the bow-shock and the flow dynamics do not allow the formation of collimated structures [24, 28, 107]. In the case of SNR G327.1-1.1 [98] have suggested the presence of a jet-torus, but photons count and resolution are not high enough to make a definite statement. Deeper observation of transitional objects are needed.

The ultimate phase of a PWN evolution depends on the pulsar kick. For slow moving pulsars the PWN will expands adiabatically inside the heated SNR, now in Sedov phase. Given the absence of energy injection, a PWN in this stage is probably only observable as a faint extended radio source, or possibly as a large TeV nebula due to IC from the relic leptons. To some extent this relic particle population might contribute to the diffuse gamma-ray background. On the contrary a fast moving pulsar can escape from the SNR, and will give rise to a bow-shock nebula due to the interaction with the ISM, through which it is moving at supersonic speeds [24,

28, 107]. These objects are observed both in $H\alpha$ emission, due to ionization of ISM neutral hydrogen, and as long extended cometary-like source of non thermal radio and X-ray emission, due to the shocked pulsar wind, now forced to flow in the direction opposite to the pulsar motion. These nebulae might constitute one of the primary sources of positrons in the galaxy.

Bow-shock PWNe, constitute a very interesting class among PWNe, and have recently received some attention, in particular regarding their X-ray emission. MHD models predict that the outflow in the tail of the bow-shock should have high speeds, of order of $0.5c$, and that the tail should form a very well collimated channel, with cross section comparable with the bow-shock size [24, 28, 107]. However observations have shown that in general the tail is wider than expected and that typical flow speed are high but of order 10000 km/s. It has been suggested that some form of mixing with the ISM, either via shear instability between the fast relativistic tail and the surrounding slower ISM, or via some particle contamination by ionized neutrals coming from the ISM, might be at play. A more detailed study of the fate of pairs injected in the tails of bow-shock nebulae, is essential, to assess the importance of pulsar as contributor to the pair CR background.

4 Conclusion

In the last few years, the combination of high resolution observations, and numerical simulations, has improved our understanding of the evolution and internal dynamics of PWNe. We can reproduce the observed jet-torus structure and we can relate the formation of the jet in the post shock flow to the wind magnetization. Simulated maps can reproduce many of the observed features, including the details of spectral properties. Results suggest that, the best agreement is achieved in the case of a wind with a large striped zone, even if MHD simulations are not able to distinguish between dissipation of the current sheet in the wind or at the TS. Results also suggest that it is possible to use X-rays imaging to constrain the pulsar wind properties; already the rings and tori observed in many PWNe have been used to determine the spin axis of the pulsar [92]. Interestingly in Crab the inner ring appear less boosted in X-rays than the optical wisps (which should trace the same flow structure) are.

Despite the undeniable successes of the MHD model, which are universally recognized within the community, and the fact that there is general agreement that the observed X-ray properties are strongly dependent on the internal dynamic at the termination shock, for reasons unknown to the author, the old KC84 model is still used as a canonical reference for interpreting observations. While this might be understandable for Radio or Optical data (where emission is quite homogeneous), it is completely unreasonable in X-ray. The fact that KC84 model is analytic and simple, is no excuse for its use, when it is clear that it is both qualitatively and quantitatively wrong, to the point that it basically fails to explain almost every single aspect of X-ray data. Moreover numerical tools and facilities are today widely available to conduct a correct study.

Interestingly, even when data are unreasonably averaged over spherical shells (even if imaging shows no hint of sphericity), they cannot be modeled using the original KC84 structure, and arbitrary velocity profiles are often assumed to reproduce the data. So one trades a model (KC84) which is wrong (nebulae are far from spherical), but at least dynamically consistent (the correct solution of MHD equations), for models which not only are wrong but also dynamically inconsistent, to the point that informations derived in this way have zero scientific valence, and the entire analysis is nothing more than a fit to the data.

There are still however unsolved questions, and possible future developments for research in this field. All present simulations are axisymmetric, and none is able to address the problem of the stability of the toroidal field, nor can they reproduce the observed emission from the jet. It is not clear if small scale disordered field is present in the inner region: maybe a residual of the dissipation in the TS of the striped wind, or an outcome of the turbulence injected by the SASI-like instability of the TS. A combination of simulations and polarimetry might help to answer this question.

Perhaps the more interesting developments might come from either the study of old systems, or from the investigation of particle energy distribution signatures in young ones. For the former, what is really needed is a large parameter study, where the various effects of pulsar proper motion and SNR reverberation are taken into account together with some simplified treatment of the spectral properties of these nebulae, in order to go beyond the simple qualitative morphological agreement, and provide templates for emission and spectral properties to be compared with observations. For the latter, a study of possible signature of different injection mechanism at the TS, either as a function of shock properties, latitude or time, should be carried on by following the full particle distribution function in the nebula, instead of the simple power-law assumption. This will allow to verify if observable signature should be expected, in what band, and provide some constrain on the physics at the TS, and more important, on relativistic shock acceleration in general.

Acknowledgements N.B. was supported by a NORDITA Fellowship grant.

References

1. Abdo, A. A., et al. 2010, ApJ, 708, 1254
2. Abdo, A. A., et al. 2010, ApJ, 714, 927
3. Amato, E., & Arons, J. 2006, ApJ, 653, 325
4. Amato, E., Salvati, M., Bandiera, R., Pacini, F., & Woltjer, L. 2000, A&A, 359, 1107
5. Amato, E., Guetta, D., & Blasi, P. 2003, A&A, 402, 827
6. Arons, J. 1998, "Neutron Star and Pulsar: Thirty years after Discovery", Proc. International Conference on Neutron Stars and Pulsars, 17-20 Nov 1997, Rikko Univ., Tokyo
7. Bandiera, R., Amato, E., & Woltjer, L. 1998, Memorie della Societa Astronomica Italiana, 69, 901
8. Bandiera, R., Amato, E., Pacini, F., Salvati, M., & Woltjer, L. 1999, Astrophysical Letters Communications, 38, 21

9. Begelman, M. C. 1998, ApJ, 493, 291
10. Begelman, M. C. 1999, ApJ, 512, 755
11. Begelman, M. C., & Li, Z.-Y. 1992, ApJ, 397, 187
12. Begelman, M. C., & Li, Z.-Y. 1994, ApJ, 426, 269
13. Beskin, V. S., Kuznetsova, I. V., & Rafikov, R. R. 1998, MNRAS, 299, 341
14. Bietenholz, M. F., Kassim, N., Frail, D. A., Perley, R. A., Erickson, W. C., & Hajian, A. R. 1997, ApJ, 490, 291
15. Bietenholz, M. F., Hester, J. J., Frail, D. A., & Bartel, N. 2004, ApJ, 615, 794
16. Blondin, J. M., Chevalier, R. A., & Frierson, D. M. 2001, ApJ, 563, 806
17. Bocchino, F., Warwick, R. S., Marty, P., Lumb, D., Becker, W., & Pigot, C. 2001, A&A, 369, 1078
18. Bogovalov, S. V. 2001, A&A, 367, 159
19. Bogovalov, S. V. 2001, A&A, 371, 1155
20. Bogovalov, S. V., & Khangoulian, D. V. 2002, MNRAS, 336, L53
21. Bogovalov, S. V., & Khangoulyan, D. V. 2002, Astronomy Letters, 28, 373
22. Bogovalov, S. V., Chechetkin, V. M., Koldoba, A. V., & Ustyugova, G. V. 2005, MNRAS, 358, 705
23. Bucciantini, N. 2002, A&A, 387, 1066
24. Bucciantini, N., & Bandiera, R. 2001, A&A, 375, 1032
25. Bucciantini, N., Blondin, J. M., Del Zanna, L., & Amato, E. 2003, A&A, 405, 617
26. Bucciantini, N., Bandiera, R., Blondin, J. M., Amato, E., & Del Zanna, L. 2004a, A&A, 422, 609
27. Bucciantini, N., Amato, E., Bandiera, R., Blondin, J. M., & Del Zanna, L. 2004b, A&A, 423, 253
28. Bucciantini, N., Amato, E., & Del Zanna, L. 2005a, A&A, 434, 189
29. Bucciantini, N., del Zanna, L., Amato, E., & Volpi, D. 2005b, A&A, 443, 519
30. Bucciantini, N., Thompson, T. A., Arons, J., Quataert, E., & Del Zanna, L. 2006a, MNRAS, 368, 1717
31. Bucciantini, N., & Del Zanna, L. 2006b, A&A, 454, 393
32. Bucciantini, N., Arons, J., & Amato, E. 2010, astro-ph/1005.1831
33. Camus, N., Komissarov, S., Bucciantini, N., & Hughes, P.A. 2009, MNRAS, 400, 1241
34. Contopoulos, I., Kazanas, D., & Fendt, C. 1999, ApJ, 511, 351
35. Camilo, F., Gaensler, B. M., Gotthelf, E. V., Halpern, J. P., & Manchester, R. N. 2004, ApJ, 616, 1118
36. de Jager, O. C. 2005, Astrophysical Sources of High Energy Particles and Radiation, 801, 298
37. de Jager, O. C., Ferreira, S. E. S., & Djannati-Ataï, A. 2008, American Institute of Physics Conference Series, 1085, 199
38. DeLaney, T., Gaensler, B. M., Arons, J., & Pivovarov, M. J. 2006, ApJ, 640, 929
39. Del Zanna, L., Bucciantini, N., & Londrillo, P. 2003, A&A, 400, 397
40. Del Zanna, L., Amato, E., & Bucciantini, N. 2004, A&A, 421, 1063
41. Del Zanna, L., Volpi, D., Amato, E., & Bucciantini, N. 2006, A&A, 453, 621
42. Dodson, R., Lewis, D., McConnell, D., & Deshpande, A. A. 2003, MNRAS, 343, 116
43. Ferreira, S. E. S., & de Jager, O. C. 2008, A&A, 478, 17
44. Gaensler, B. M., Pivovarov, M. J., & Garmire, G. P. 2001, ApJL, 556, L107
45. Gaensler, B. M., Arons, J., Kaspi, V. M., Pivovarov, M. J., Kawai, N., & Tamura, K. 2002, ApJ, 569, 878
46. Gaensler, B. M., & Slane, P. O. 2006, ARA&A, 44, 17
47. Gallant, Y. A., & al. 2007, "VHE gamma-ray emitting pulsar wind nebulae discovered by HESS", these proceedings
48. Gammie, C. F., McKinney, J. C., & Tóth, G. 2003, ApJ, 589, 444
49. Gelfand, J. D., Slane, P. O., & Zhang, W. 2009, ApJ, 703, 2051
50. Gotthelf, E. V., & Wang, Q. D. 2000, ApJL, 532, L117
51. Gruzinov, A. 2005, Physical Review Letters, 94, 021101
52. Helfand, D. J., Gotthelf, E. V., & Halpern, J. P. 2001, ApJ, 556, 380
53. Hester, J. J. 2008, ARA&A, 46, 127

54. Hester, J. J., et al. 1995, *ApJ*, 448, 240
55. Hester, J. J., et al. 1996, *ApJ*, 456, 225
56. Hester, J. J., et al. 2002, *ApJL*, 577, L49
57. Hickson, P., & van den Bergh, S. 1990, *ApJ*, 365, 224
58. Hoffmann, A. I. D., Horns, D., & Santangelo, A. 2007, *A&SS*, 309, 215
59. Horns, D., Aharonian, F., Santangelo, A., Hoffmann, A. I. D., & Masterson, C. 2006, *A&A*, 451, L51
60. Jun, B.-I. 1998, *ApJ*, 499, 282
61. Kargaltsev, O., & Pavlov, G. G. 2007, "Pulsar wind nebulae in the CHANDRA era", AIP Conference Proceedings 983, 171
62. Kargaltsev, O., Pavlov, G. G., Misaniivic, Z., & Garmire, G. P. 2007, "X-ray observation of pulsar tails", these proceedings.
63. Khangoulain, D. V., & Bogovalov, S. V. 2003, *Astronomy Letters*, 29, 495
64. Kennel, C. F., & Coroniti, F. V. 1984, *ApJ*, 283, 710, KC84
65. Kennel, C. F., & Coroniti, F. V. 1984, *ApJ*, 283, 694, KC84
66. Kirk, J. G., & Skjæraasen, O. 2003, *ApJ*, 591, 366
67. Komissarov, S. S. 1999, *MNRAS*, 303, 343
68. Komissarov, S. S. 2006, *MNRAS*, 367, 19
69. Komissarov, S. S., & Lyubarsky, Y. E. 2004, *MNRAS*, 349, 779
70. Kothes, R., Reich, W., & Uyaniker, B. 2006, *ApJ*, 638, 225
71. Kramer, M. 2007, "Observation of pulsed emission from pulsars", these proceedings
72. Melatos, A., et al. 2005, *ApJ*, 633, 931
73. Lemoine-Goumard, M., private communication, these proceedings
74. Lu, F. J., Wang, Q. D., Aschenbach, B., Durouchoux, P., & Song, L. M. 2002, *ApJL*, 568, L49
75. Lyubarsky, Y. E. 2002, *MNRAS*, 329, L34
76. Lyubarsky, Y. E. 2003, *MNRAS*, 345, 153
77. Lyubarsky, Y. 2005, *Advances in Space Research*, 35, 1112
78. Lyubarsky, Y., & Eichler, D. 2001, *ApJ*, 562, 494
79. Lyubarsky, Y., & Kirk, J. G. 2001, *ApJ*, 547, 437
80. Lyutikov, M. 2003, *MNRAS*, 339, 623
81. Michel, F. C. 1973, *ApJL*, 180, L133
82. Michel, F. C., Scowen, P. A., Dufour, R. J., & Hester, J. J. 1991, *ApJ*, 368, 463
83. Mori, K., Burrows, D. N., Hester, J. J., Pavlov, G. G., Shibata, S., & Tsunemi, H. 2004, *ApJ*, 609, 186
84. Mori, K., Burrows, D. N., Pavlov, G. G., Hester, J. J., Shibata, S., & Tsunemi, H. 2004b, *IAU Symposium*, 218, 181
85. Ng, C.-Y., Slane, P. O., Gaensler, B. M., & Hughes, J. P. 2008, *ApJ*, 686, 508
86. Pavlov, G. G., Kargaltsev, O. Y., Sanwal, D., & Garmire, G. P. 2001, *ApJL*, 554, L189
87. Pavlov, G. G., Teter, M. A., Kargaltsev, O., & Sanwal, D. 2003, *ApJ*, 591, 1157
88. Rees, M. J., & Gunn, J. E. 1974, *MNRAS*, 167, 1
89. Reynolds, S. P., & Chevalier, R. A. 1984, *ApJ*, 278, 630
90. Roberts, M. S. E., Gotthelf, E. V., Halpern, J. P., Brogan, C. L., & Ransom, S. M. 2006, *arXiv:astro-ph/0612631*
91. Romani, R. W., & Ng, C.-Y. 2003, *ApJL*, 585, L41
92. Romani, R. W., Ng, C.-Y., Dodson, R., & Brisken, W. 2005, *ApJ*, 631, 480
93. Schmidt, G. D., Angel, J. R. P., & Beaver, E. A. 1979, *ApJ*, 227, 106
94. Shibata, S., Tomatsuri, H., Shimanuki, M., Saito, K., & Mori, K. 2003, *MNRAS*, 346, 841
95. Slane, P., Helfand, D. J., van der Swaluw, E., & Murray, S. S. 2004, *ApJ*, 616, 403
96. Spitkovsky, A. 2006, *ApJL*, 648, L51
97. Spitkovsky, A., & Arons, J. 2004, *ApJ*, 603, 669
98. Temim, T., Slane, P., Gaensler, B. M., Hughes, J. P., & Van Der Swaluw, E. 2009, *ApJ*, 691, 895
99. Truelove, J. K., & McKee, C. F. 1999, *ApJSup.*, 120, 299
100. Trussoni, E., Massaglia, S., Bodo, G., & Ferrari, A. 1988, *MNRAS*, 234, 539
101. van der Swaluw, E. 2003, *A&A*, 404, 939

102. van der Swaluw, E., Achterberg, A., Gallant, Y. A., & Tóth, G. 2001, *A&A*, 380, 309
103. van der Swaluw, E., Achterberg, A., Gallant, Y. A., Downes, T. P., & Keppens, R. 2003, *A&A*, 397, 913
104. van der Swaluw, E., Downes, T. P., & Keegan, R. 2004, *A&A*, 420, 937
105. Veron-Cetty, M. P., & Woltjer, L. 1993, *A&A*, 270, 370
106. Velusamy, T. 1985, *MNRAS*, 212, 359
107. Vigelius, M., Melatos, A., Chatterjee, S., Gaensler, B. M., & Ghavamian, P. 2007, *MNRAS*, 374, 793
108. Volpi, D./ 2006, Thesis: “La Struttura Interna della Nebulosa del Granchio”
109. Volpi, D., Del Zanna, L., Amato, E., & Bucciantini, N. 2008, *A&A*, 485, 337
110. Weisskopf, M. C., et al. 2000, *ApJL*, 536, L81
111. Willingale, R., Aschenbach, B., Griffiths, R. G., Sembay, S., Warwick, R. S., Becker, W., Abbey, A. F., & Bonnet-Bidaud, J.-M. 2001, *A&A*, 365, L212
112. Wilson, A. S. 1972, *MNRAS*, 157, 229